Porous Gold-Nanoparticle−$CaCO_3$ Hybrid Material: Preparation, Characterization, and Application for Horseradish Peroxidase Assembly and Direct Electrochemistry

Wen-Yi Cai,[†] Qin Xu,[†] Xiao-Ning Zhao,[‡] Jun-Jie Zhu,*[,†] and Hong-Yuan Chen[†]

Department of Chemistry, Key Lab of Analytical Chemistry for Life Science, Nanjing University, Nanjing 210093, PR China, and Department of Physics, Nanjing University, Nanjing 210093, PR China

Received July 3, 2005. Revised Manuscript Received November 17, 2005

Gold nanoparticles (AuNPs) were assembled on the surface of porous calcium carbonate microspheres ($CaCO_3$) in a neutral aqueous solution through electrostatic interaction. The resulting gold-nanoparticle−$CaCO_3$ hybrid material (AuNP−$CaCO_3$) was characterized and expected to offer a promising template for enzyme immobilization and biosensor fabrication because of its satisfying biocompatibility and improved properties. It was conjugated with horseradish peroxidase (HRP) to fabricate HRP−AuNP−$CaCO_3$ bioconjugates, which were then embedded into a silica sol−gel matrix to construct a novel biosensor. Because of the synergic effect of $CaCO_3$ microspheres and AuNPs, direct electron transfer of HRP was observed at this biosensor. The biosensor exhibited a fast amperometric response to H_2O_2, with a linear range of 4.0×10^{-5} to 8.0×10^{-3} mol/L. The detection limit was 1.0×10^{-6} mol/L based on $S/N = 3$.

Introduction

The development of materials science has brought a great momentum to bioelectroanalysis. Analysts in this field are always enthusiastic in finding new materials with good biocompatibility for improving the behavior of biosensors. Metal nanoparticles, for example, once used in electrochemical biosensors, could act as nanoelectrodes that communicate electrons from an enzyme redox site to a macroscopic electrode, thus leading to a novel class of enzyme electrodes.[1] Inorganic porous materials, especially silica-based materials, can be used as an efficient support for enzyme loading[2] and have already been widely used in biosensor fabrication.[3] Recently, a growing interest in non-silica-based porous structured materials has sparked contributions, probably because of their potentially valuable applications in areas such as biosenors, drug delivery, microreactors, and bioseparations.[4]

Calcium carbonate, a natural mineral with great biocompatibility, has been proven to intensify enzyme performance[5] and has been widely used in industry, technology, medicine, microcapsule fabrication, and many other bio-related fields.[6] It can be precipitated as three distinct crystalline phases: calcite, aragonite, and vaterite.[7] The spherical vaterite polymorph, often composed of nanoparticles with diameters of 10−30 nm, is expected to be used for various purposes because of its specific features, such as a higher surface area, better dispersibility in water, and smaller specific gravity than the other two crystal systems.[8] Recently, it has also been used for enzyme immobilization because of its porous structure and good biocompatibility.[6] However, although vaterite is stable under dry conditions, when in contact with water, it transforms easily and irreversibly into the thermodynamically stable calcite,[8] which greatly hinders its application.

A coating method is often used to fabricate hybrid materials with multifunctional and improved properties. The resulting core−shell structures with specific catalytic, magnetic, electronic, or optical properties could be widely used in fields such as electronics, magnetism, optics, and catalysis.[9,10] In this work, citrate-stabilized gold nanoparticles (AuNPs) were assembled on the surface of porous carbonate microspheres to fabricate a AuNP−$CaCO_3$ hybrid material. This material retained the porous structure and inherited the advantages from its parent materials, such as satisfying biocompatibility and good solubility and dispersibility in water. Meanwhile, it was found to be superior because of its improved stability under wet conditions.

Like the core−shell AuNP−polyurethane material,[11] this multifunctional material could provide a biocompatible

* To whom correspondence should be addressed. Fax: 86-25-3317761. Tel: 86-25-3594976. E-mail: jjzhu@netra.nju.edu.cn.

[†] Department of Chemistry, Key Lab of Analytical Chemistry for Life Science, Nanjing University.

[‡] Department of Physics, Nanjing University.

(1) Katz, E.; Willner, I.; Wang, J. *Electroanalysis* **2004**, *16*, 19−44.
(2) (a) Wang, Y.; Caruso, F. *Chem. Commun.* **2004**, 1529. (b) Wang, Y.; Caruso, F. *Chem. Mater.* **2005**, *17*, 953. (c) Wang, Y.; Yu, A.; Caruso, F. *Angew. Chem., Int. Ed.* **2005**, *44*, 2888.
(3) Dai, Z. H.; Xu, X. X.; Ju, H. X. *Anal. Biochem.* **2004**, *332*, 23−31.
(4) (a) Shchukin, D.; Shutava, T.; Sukhorukov, G.; Lvov, Y. M. *Chem. Mater.* **2004**, *16*, 3446. (b) Zhu, H.; Stein, E. W.; Lu, Z.; Lvov, Y. M.; McShane, M. J. *Chem. Mater.* **2005**, *17*, 2323.
(5) Rosu, R.; Iwasaki, R.; Shimizu, N.; Doisaki, N.; Yamane, T. *J. Biotechnol.* **1998**, *66*, 51−59.
(6) Volodkin, D. V.; Larionova, N. I.; Sukhorukov, G. B. *Biomacromolecules* **2004**, *5*, 1962−1972.
(7) Falini, G.; Fermani, S.; Gazzano, M.; Ripamonti, *A. Chem.−Eur. J.* **1998**, *4*, 1048−1052.
(8) Naka, K.; Tanaka, Y.; Chujo, Y. *Langmuir* **2002**, *18*, 3655−3658.
(9) Ji, T. H.; Lirtsman, V. G.; Avny, Y.; Davidov, D. *Adv. Mater.* **2001**, *13*, 1253−1256.
(10) Sun, X. M.; Li, Y. D. *Angew. Chem., Int. Ed.* **2004**, *43*, 597−601.

10.1021/cm051442i CCC: $33.50
Published on Web 12/22/2005

Scheme 1. Process of Fabricating HRP−AuNP−$CaCO_3$ Bioconjugates

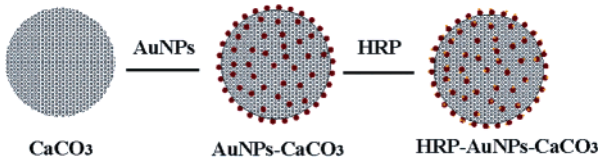

surface for enzyme loading (Scheme 1). The resulting enzyme−AuNP−$CaCO_3$ bioconjugates could find their application in bioelectroanalysis. We have already reported the direct electron-transfer properties of horseradish peroxidase (HRP) on the bioconjugate-modified glassy carbon electrode in a recent communication.[10] In this paper, we detail the properties of the hybrid material and the performance of the biosensor. The biosensor showed a fast amperometric response to H_2O_2, with a linear range 4.0×10^{-5}−8.0×10^{-3} mol/L. The detection limit was 1.0×10^{-6} mol/L based on $S/N = 3$.

Experimental Section

Chemicals and Apparatus. HRP (250 units/mg) was obtained from Sino-American Biotechnology Corp. (Hebei, China) and was used without further purification. H_2O_2 (30% w/v solution), $CaCl_2 \cdot 2H_2O$, Na_2CO_3, and $HAuCl_4 \cdot 4H_2O$ were purchased from Shanghai Chemical Reagent Co. (Shanghai, China). Tetraethyl orthosilicate (TEOS) was obtained from Tianjin Reagent Factory (Tianjin, China). All other chemicals were of analytical grade. All the solutions were prepared with doubly distilled water.

UV−vis and diffuse reflectance (DRS) spectra were recorded on a Shimadzu UV-2100 recording spectrophotometer at room temperature. $BaSO_4$ was used as the reference for DRS. Transmission electron micrographs (TEM) were recorded on a JEOLJEM 200CX transmission electron microscope, using an accelerating voltage of 200 kV. Ultrathin sections of the AuNP−$CaCO_3$ hybrid materials (30−100 nm in thickness) were obtained using a Power Tome XL ultracut UCT ultramicrotome after setting the sample in an LR−White resin. The thin sections were then placed on noncoated copper grids and characterized with a high-resolution transmission electron microscope (HRTEM) (Technai F 20 s-twin, FEI Co., Hillsboro, OR at an accelerating voltage of 200 kV. Scanning electron microscopic (SEM) measurements were carried out on a JSM-5610/LV scanning electron microscope (Thermo NORAN) at 15 kV. Brunauer−Emmett−Teller (BET) data were collected with a Micromeritics-ASAP 2020 surface area and porosity analyzer at 77 K. The BET surface area was calculated from the linear part of the BET plot. The pore-size distribution plots are obtained by using the Barrer−Jovner−Halenda (BJH) model.

Amperometric, cyclic voltammetric, and electrochemical impedance experiments were performed using a CHI660B workstation (Shanghai Chenhua, Shanghai, China). All experiments were carried out using a conventional three-electrode system with the enzyme electrode as the working electrode, a platinum wire as the auxiliary electrode, and a saturated KCl electrode as the reference electrode. The electrochemical impedance measurements were carried out in a background solution of 5 mM $K_3Fe(CN)_6 + K_4Fe(CN)_6$ in 0.1 M KCl at a bias potential of 0.24 V. The alternative voltage was 5 mV, and the frequency range was 1 Hz−100 kHz. Electrolyte solutions were purged with high-purity nitrogen prior to and blanketed with nitrogen during electrochemical experiments.

Preparation of Gold Nanoparticles and $CaCO_3$ Microspheres. Gold nanoparticles were prepared according to the literature[12,13] by adding a sodium citrate solution to a boiling $HAuCl_4$ solution. The molar ratio of $HAuCl_4$:sodium citrate used for the preparation of the colloid was 0.75. The diameter of the prepared AuNPs was ca. 25 nm, which was measured using transmission electron microscopy. $CaCO_3$ microspheres were prepared by rapidly pouring a 0.33 M Na_2CO_3 solution into an equal volume of a 0.33 M solution of $CaCl_2$ at room temperature on a magnetic stirrer.[4] The precipitate was centrifuged, washed with pure water, and dried.

Preparation of AuNP−$CaCO_3$ Hybrid Material. $CaCO_3$ (0.5 g) was dispersed in 50 mL of a Au colloid solution (pH 7) and sonicated for 20 min. After centrifugation, the light purple AuNP−$CaCO_3$ composites were obtained; the supernatant liquor was colorless. The composites were further washed with distilled water three times and dried.

Preparation of HRP−AuNP−$CaCO_3$ Bioconjugates. The hybrid material (10 mg) prepared above was dispersed in a solution of HRP (1 mg/mL, pH 7) and shaken for 1 h for enzyme absorption. The bioconjugates were then centrifuged and washed with distilled water three times.

The UV−vis spectrum was used to monitor the concentrations of the gold colloid and HRP solutions before and after the assembly process. The decreases in absorbance of the two solutions were applied to quantify the loading amount of AuNPs and HRP bound to the $CaCO_3$ microspheres; the bands used were 527 and 402 nm, respectively.

The leakage of the AuNPs was monitored by a 180-80 (Hitachi) atomic absorption spectrometer (AAS). The AuNP−$CaCO_3$ hybrid material was dispersed in water for about 20 days. The supernatant obtained after centrifugation of the hybrid material was then analyzed.

Preparation of Silica Sol. Silica sol was prepared according to the literature[14] by mixing 600 μL of ethanol, 50 μL of TEOS, 10 μL of 5 mM NaOH, and 60 μL of H_2O in a small test tube at room temperature. After being sonicated, the sol was formed and stored at 4 °C.

Fabrication of the Biosensor. A glassy carbon electrode (GCE) was polished successively with 1.0, 0.3, and 0.05 μm alumina powder; it was rinsed thoroughly with doubly distilled water between each polishing step. Next, the polished electrode was sonicated in acetone and doubly distilled water and was then allowed to dry at room temperature. The HRP−AuNP−$CaCO_3$ bioconjugates obtained above were resuspended in 0.5 mL of water, and 10 μL of this suspension was deposited on the surface of the pretreated GCE. It was then left to dry at room temperature. Silica sol (10 μL) was then added for encapsulation of the bioconjugates. The electrode was then left to dry and was stored for at least 24 h at 4 °C. The biosensor was stored under the same conditions when not in use.

The AuNP−$CaCO_3$/silica sol−gel-modified GCE and $CaCO_3$/silica sol−gel-modified GCE were fabricated using the same GCE by the same method except that AuNP−$CaCO_3$ or $CaCO_3$ was used instead of the bioconjugates. For the silica sol−gel-modified GCE, the surface of the glassy carbon electrode was covered by 10 μL of silica sol, and the electrode was then allowed to dry at room temperature.

(11) Phadtare, S.; Kumar, A.; Vinod, V. P.; Dash, C.; Palaskar, D. V.; Rao, M.; Shukla, P. G.; Sivaram, S.; Sastry, M. *Chem. Mater.* **2003**, *15*, 1944−1949.

(12) Xu, Q.; Cai, W. Y.; Zhu, J. J. *Chem. Lett.* **2005**, *34*, 832−834.

(13) Turkevich, J.; Stevenson, P. C.; Hiller, J. *Faraday Discuss.* **1951**, *11*, 55−75.

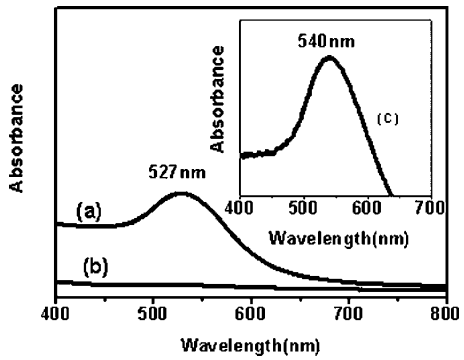

Figure 1. UV−vis spectra recorded from (a) the Au colloid solution and (b) the gold solution after sonication with $CaCO_3$ for 20 min and centrifugation. The inset is the diffuse reflectance spectra of the AuNP−$CaCO_3$ composites.

Results and Discussion

Preparation and Characterization of the AuNP−$CaCO_3$ Hybrid Material. Porous $CaCO_3$ microspheres have already been used as templates for enzyme immobilization. The presence of nanometer-sized pores and channels in $CaCO_3$ particles offered a great opportunity for capturing biomacromolecules such as proteins via physical adsorption/pore diffusion, thus enabling very high substrate loading.[6] In our work, the same effect took place. With the isoelectric point (IEP) at pH 8.5,[6] $CaCO_3$ microspheres were positively charged at pH 7.0 whereas AuNPs were negatively charged at the same pH. The electrostatic interaction caused the assembly of AuNPs on the surface of the oppositely charged $CaCO_3$ microspheres; the unique structure of $CaCO_3$ microspheres greatly facilitated this assembly process.

The process was monitored by UV−vis spectroscopy. Figure 1 shows the UV−vis spectra of the prepared colloidal gold solution (a) and the gold solution after being sonicated with $CaCO_3$ for 20 min and centrifuged (b). A great loss in the intensity of the surface plasmon resonance could be found at 527 nm after the AuNPs were assembled, which indicated the absorption of the AuNPs on the $CaCO_3$ surface. Meanwhile, the diffuse reflectance spectra of the AuNP−$CaCO_3$ composite (Figure 1 inset) showed an absorption band centered at 540 nm, indicating capture of AuNPs. The shift in the resonance wavelength indicated aggregation of the gold nanoparticles on the $CaCO_3$ surface.[9] From the loss of intensity at 527 nm in this figure, we made a rough estimate of 0.2% for the mass loading of $CaCO_3$ microspheres with gold nanoparticles.

Figure 2 shows the TEM images of both $CaCO_3$ (a) and the AuNP−$CaCO_3$ hybrid material (b) and the HRTEM images of the hybrid material (c, d). The AuNPs decorating the surface of the $CaCO_3$ microspheres can be clearly observed in Figure 2B. HRTEM images of the ultramicrotome spheres were used to obtain information about the inner structures of the hybrid material and the presence and distribution of the Au nanoparticles in the $CaCO_3$ particles. Panels c and d of Figure 2 clearly demonstrate the spherical shapes and channel-like interior structures of the hybrid materials. The high-magnification (Figure 2D inset) image confirmed that AuNPs were present in the $CaCO_3$ microspheres.

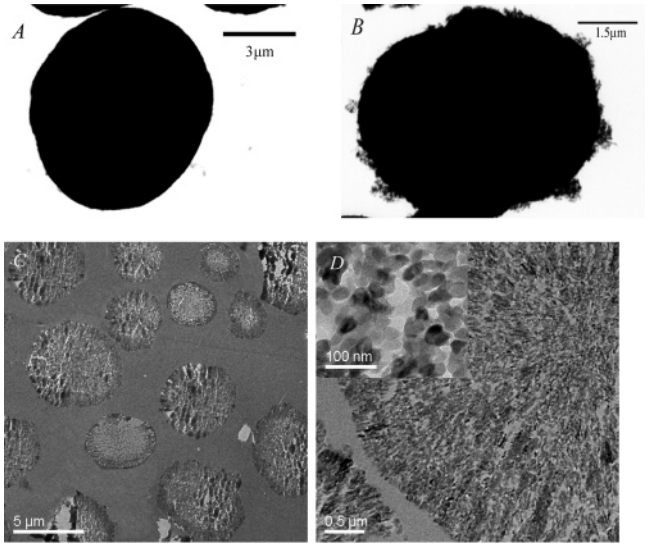

Figure 2. TEM images of (a) $CaCO_3$ microspheres and (b) AuNP−$CaCO_3$ microspheres. HRTEM images of ultramicrotome thin sections of AuNP−$CaCO_3$ spheres at (c) low and (d) high magnification. The inset of d is a magnification that indicated the presence of AuNPs in the $CaCO_3$ particles.

SEM images of both $CaCO_3$ microspheres and the AuNP−$CaCO_3$ hybrid material are shown in Figure 3. The surface of the prepared $CaCO_3$ microspheres (Figure 3A) was rough and consisted of a great number of carbonate nanoparticles. These nanoparticles were combined to form the specific morphology.[4] This unique structure played an important role in the AuNP assembly. The assembly of the AuNPs resulted in a smooth surface texture for the hybrid material, as shown in Figure 3B. Figure 3C exhibits the SEM image of a broken particle of the hybrid material at higher magnification. Although a smooth surface texture after AuNP loading indicated a decrease in pore size, the interior channel-like structure was retained. In a contrast experiment, the poor ability of calcite (Figure 3D) to accommodate AuNPs was proven when calcite replaced the vaterite template for adsorbing AuNPs. The color of the resulting deposit was nearly white after centrifugation and washing, indicating that calcite could not parallel vaterite as a template for AuNP loading because of its different structure.

The Brunauer−Emmett−Teller (BET) method of nitrogen adsorption/desorption was further used to characterize the surface area, pore volume, and pore-size distribution of $CaCO_3$ microspheres before and after AuNP absorption. The N_2 absorption isotherms in Figure 4 showed a decrease in surface area after AuNP loading. BET analysis revealed a surface area of 7.26 m^2/g for $CaCO_3$ (Figure 4a) and 5.59 m^2/g for the AuNP−$CaCO_3$ hybrid material (Figure 4b). Meanwhile, the hybrid material had a pore volume of 0.097 cm^3/g, which was smaller than that of the $CaCO_3$ microspheres (0.136 cm^3/g). In the inset of Figure 4, a narrower pore-size distribution and a sharp decrease in the number of larger pores were observed because of the infiltration of the AuNPs into the $CaCO_3$ microspheres. Although the AuNPs could not penetrate into small pores because of steric difficulties, they could still infiltrate into some larger ones. With AuNPs filling in larger pores, these pores became smaller, resulting in a decrease in the whole pore volume as well as the BET surface area.

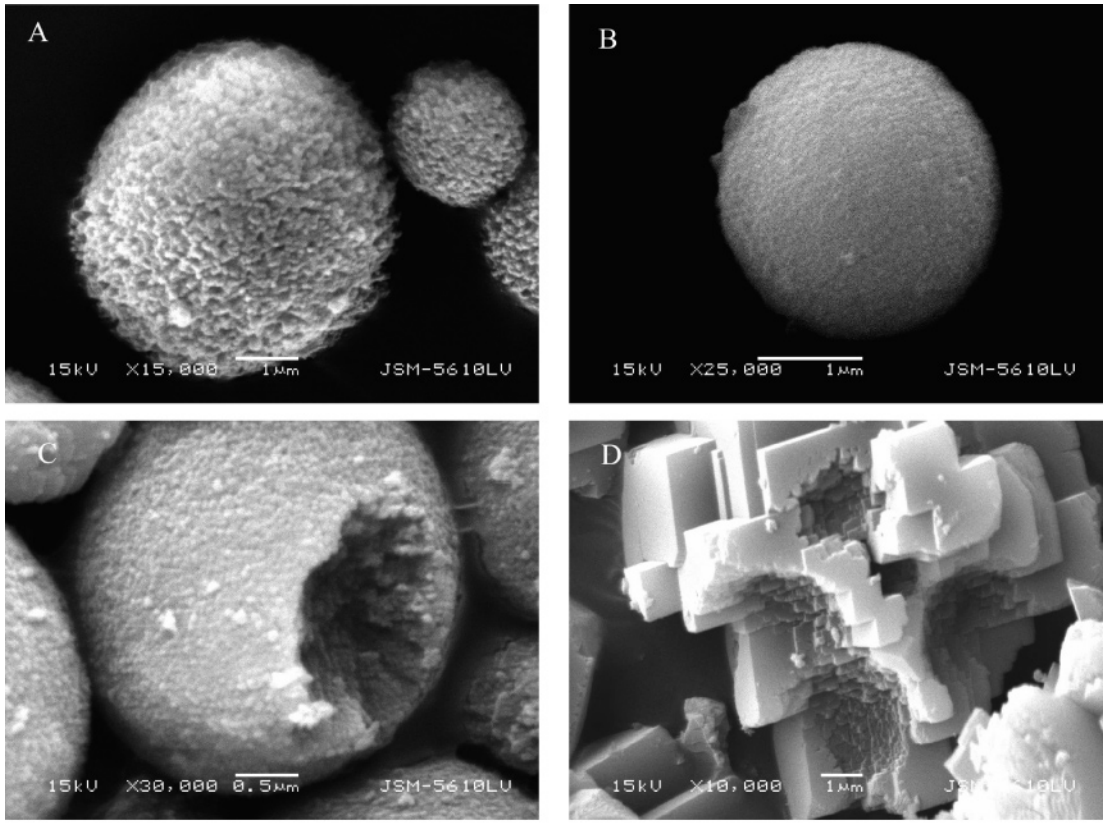

Figure 3. SEM images of (a) $CaCO_3$ microparticles, (b) AuNP−$CaCO_3$ hybrid material, (c) a broken particle of the AuNP−$CaCO_3$ composite, and (d) calcite acquired after the recrystallization of vaterite.

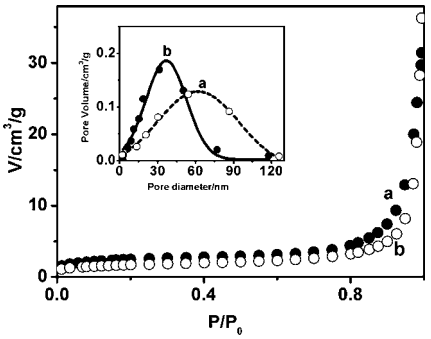

Figure 4. N_2 absorption isotherms of (a) $CaCO_3$ and (b) AuNP−$CaCO_3$. Inset is the pore size distribution of (a) $CaCO_3$ and (b) AuNP−$CaCO_3$.

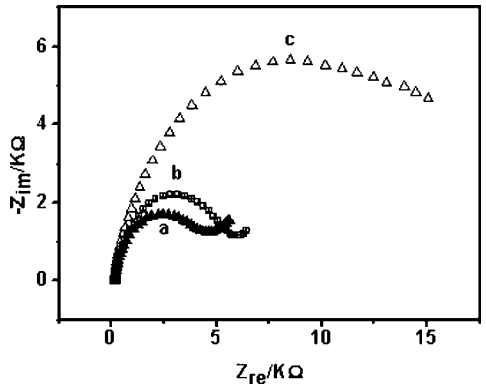

Figure 5. Nyquist plot of electrochemical impedance spectroscopy for (a) AuNP−$CaCO_3$/silica sol−gel-modified GCE, (b) $CaCO_3$/silica sol−gel-modified GCE, and (c) silica sol−gel-modified GCE.

The hybrid material inherited advantages from its parent materials, such as satisfying biocompatibility and good solubility and dispersibility in water, and was expected to be a promising template for enzyme loading and biosensing. Furthermore, it has the ability to facilitate electron transfer in a silica sol−gel matrix, and electrochemical impedance experiments were performed to verify this. The use of silica sol−gel-monolith-based electrochemical biosensors has been hindered by the nonconducting nature of the sol−gel matrix;[14,15] therefore, many improvements have been made to its performance. Mediators such as ferrocene[15] and conductive material such as graphite microparticles[16] are typical examples of compounds used to solve this problem.

In the present work, the AuNP−$CaCO_3$ hybrid material could play a role similar to that of ferrocene and graphite microparticles. Figure 5 showed the Nyquist plot of electrochemical impedance spectroscopy for both the $CaCO_3$/silica sol−gel-modified and AuNP−$CaCO_3$/silica sol−gel-modified GCEs. The semicircle portion at higher frequencies included in the impedance spectra corresponded to the electron-transfer-limited process. The diameter of the semicircle corresponded to the electrotransfer resistance (R_{et}), which controlled the electron-transfer kinetics of the redox probe at the electrode interface.[17] Both electrodes showed large decreases in diameter compared to that of the silica sol−gel-modified electrode, indicating much lower R_{et}

(14) Wang, Q. L.; Lu, G. X.; Yang, B. J. *Biosens. Bioelectron.* **2004**, *19*, 1269−1275.
(15) Chut, S. L.; Li, J.; Tan, N. *Analyst* **1997**, *122*, 1431−1434.
(16) Coche-Gue'rente, L.; Cosnier, S.; Labbe, P. *Chem. Mater.* **1997**, *9*, 1348−1352.
(17) Xu, J. Z.; Zhu, J. J.; Huang, Q.; Chen, H. Y. *Electrochem. Commun.* **2001**, *3*, 665−669.

values. It can be thought that $CaCO_3$ microspheres and AuNPs do not retard but instead enhance the rate of electron transfer.[18] The electrode modified with AuNP−$CaCO_3$ showed a lower R_{et} compared to that of a $CaCO_3$-based electrode because of the contribution of assembled AuNPs.

The advantages of the hybrid material made it suitable for enzyme loading. In our experiment, HRP was used as a simple model to study the feasibility of using this material in bioelectroanalysis. With the PI at 8.8,[19] HRP was positively charged at pH 7.0, and thus could easily assemble on this hybrid material because of electrostatic interactions and interactions between AuNPs and the amine groups of the enzyme. A smaller BET surface area (2.62 m^2/g) and smaller pore volume (0.0089 cm^3/g) for HRP−AuNP−$CaCO_3$ bioconjugates compared to those values for the AuNP−$CaCO_3$ hybrid material indicated the loading of HRP. Because of its small size ($6.0 \times 3.5 \times 3.0$ nm^3),[6] HRP molecules could penetrate into most of the pores, resulting in a decrease in the pore volume, as shown in Figure 4c. Calculating the difference in the concentration of the enzyme before and after adsorption, we found that about 25 μg of HRP was captured by 1 mg of $CaCO_3$ particles from a protein solution with a concentration of 1 mg/mL of HRP.

Compared with $CaCO_3$ microspheres in the absence of AuNPs, the hybrid material seems to be superior because of its improved stability in aqueous solution. When the hybrid material was conjugated with HRP and kept in water for 20 days, vaterite was still the dominant polymorph. On the other hand, gold could not be detected in the supernatant liquid by AAS (detection sensitivity in parts per million (ppm)), clearly showing that the AuNPs were strongly absorbed on the surface of $CaCO_3$ microspheres. In contrast, when $CaCO_3$ microspheres were conjugated with HRP in the absence of AuNPs and stored in water overnight, calcite became the dominant polymorph (see the Supporting Information). It seemed that AuNPs, which decorated not only the surface but also the inside of the vaterite microsphere pores, prevented the leakage of Ca^{2+} and CO_3^{2-}, which would result in recrystallization.[6]

Direct Electrochemistry of the HRP−AuNP−$CaCO_3$ Bioconjugate-Modified Electrode. The HRP−AuNP−$CaCO_3$ bioconjugate offered a novel type of biocatalyst for biosensor fabrication. A biosensor based on it was fabricated to test its feasibility in biosensing. Figure 6 shows cyclic voltammograms (CVs) of the bioconjugate-modified electrode in a 0.1 M PBS (pH 7.0) solution at 100 mV/s (Figure 6c) and the electrode modified with the AuNP−$CaCO_3$ hybrid material (Figure 6a). The hybrid-material-modified electrode exhibited no redox peaks in the potential window, indicating electro-inactiveness. The bioconjugate-modified electrode exhibited a pair of redox peaks at −0.03 and −0.118 V, which was related to the redox of the immobilized HRP. This potential was lower than the potential of the Fe(III/II) redox couple of free HRP in solution.[20] The low redox potential might imply special interactions between the molecular 3D structure of HRP and the morphology of the composite, which could strongly affect the heme microenvironment. When HRP was directly adsorbed on the surface of $CaCO_3$ microspheres, direct electron transfer of HRP could also be obtained, as shown in Figure 6b. It has been reported that the presence of some cations may promote the heterogeneous electron transfer;[21] therefore, the presence of Ca^{2+} might accelerate the electron transfer. However, such a kind of biosensor was not stable. Just as we have mentioned above, without the protection of AuNPs, HRP−$CaCO_3$ bioconjugates are not stable in aqueous solution and could transform into a rhombohedral calcite polymorphy (see the Supporting Information). As calcite was poor at accommodating protein, the peak current decayed gradually and disappeared in the end. Therefore, the direct and stable electron transfer of HRP was suggested to be the result of the synergic effect of both $CaCO_3$ and AuNPs. The hybrid material provided a biocompatible environment for HRP to orient the heme edge toward its electron donor or acceptor and facilitate its electron-transfer process.[22]

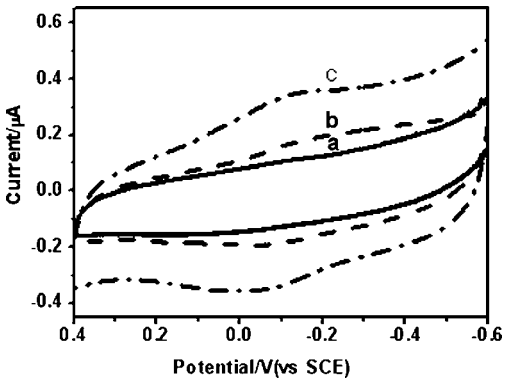

Figure 6. Cyclic voltammograms obtained with (a) AuNP−$CaCO_3$/silica sol−gel-modified GCE, (b) HRP−$CaCO_3$/silica sol−gel-modified GCE, and (c) HRP−AuNP−$CaCO_3$/silica sol−gel-modified GCE in 0.1 mol/L PBS (pH 7.0) at 100 mV/s.

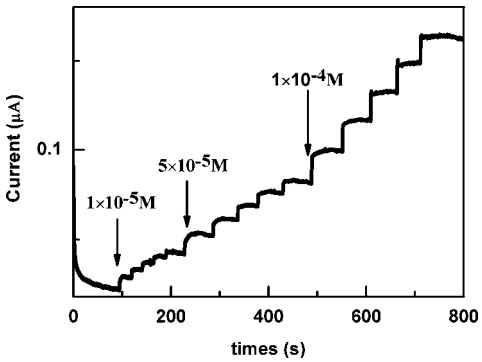

Figure 7. Typical steady-state response of the biosensor on successive injection of different concentrations of H_2O_2 into 0.1 M PBS (pH 7.0) while stirring, with an applied potential of −0.3 V.

To further investigate the bioactivity of immobilized HRP, we used this biosensor for the determination of H_2O_2. Figure 7 shows a typical response curve for the biosensor at optimized conditions on successive injections of H_2O_2 to stirring PBS at pH 7.0, and Figure 8 shows the calibration

(18) Liu, Y. J.; Li, Y. L.; Liu, S. C.; Li, J.; Yao, S. Z. *Biomaterials* **2004**, *25*, 5725−5733.
(19) Ferapontova, E. E. *Electroanalysis* **2004**, *16*, 1101−1112.
(20) Harbury, H. A. *J. Biol. Chem.* **1957**, *225*, 1009.
(21) Armstrong, F. A.; Hill, H. A. O.; Oliver, B. N.; Walton, N. J. *J. Am. Chem. Soc.* **1984**, *106*, 921.
(22) Albery, W. J.; Eddowes, M. J.; Hill, H. A. O.; Hillman, A. R. *J. Am. Chem. Soc.* **1981**, *103*, 3904.

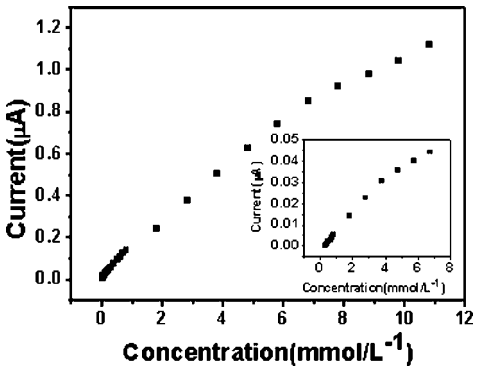

Figure 8. Calibration curves of HRP−AuNP−$CaCO_3$/silica sol−gel-modified GCE and AuNP−$CaCO_3$/silica sol−gel-modified GCE (insert curve).

curve. A clearly defined reduction current proportional to the hydrogen peroxide concentration was observed. The biosensor achieved 95% of the steady-state current within 5 s, with a linear range of 4×10^{-5} to 8×10^{-3} mol/L. The detection limit was 1×10^{-6} mol/L based on $S/N = 3$. When the biosensor was stored in a dry state at 4 °C and measured every day, the current response for 0.1 mM H_2O_2 decreased by only about 6% of the original value after 20 days. On the other hand, there is an unnoticeable change with 0.1 mM H_2O_2 after 5 h of continuous operation. The long lifetime of the biosensor may be attributed to the strengthened biocompatibility and stability of the hybrid material.

Conclusion

In this paper, $CaCO_3$ microspheres, biocompatible and typical inorganic porous natural minerals, were used for AuNP assembly. The resulting multifunctional AuNP−$CaCO_3$ hybrid material was then used for HRP assembly and biosensor fabrication to evaluate the feasibility of using this material in bioelectroanalysis. Direct electron transfer of HRP on the biosensor was observed and studied.

Acknowledgment. This work is supported by the National Natural Science Foundation of China (Grants 20325516 and 20575026), 973 Project (2004CB520804), and Jiangsu Scientific Project (BK2004210). The authors are also grateful to Mr. Ke-Yu Wang from the Modern Analytic Centre at Nanjing Normal University for extending his facilities to us.

Supporting Information Available: SEM images of the HRP−AuNP−$CaCO_3$ bioconjugate after incubation in water for 20 days and HRP−$CaCO_3$ after incubation in water for 1 day (pdf). This material is available free of charge via the Internet at http://pubs.acs.org.

CM051442I